

Modeling and Inversion of Magnetic Anomalies Caused by Sediment–Basement Interface Using Three-Dimensional Cauchy-Type Integrals

Hongzhu Cai and Michael S. Zhdanov

Abstract—This letter introduces a new method for the modeling and inversion of magnetic anomalies caused by crystalline basements. The method is based on the 3-D Cauchy-type integral representation of the magnetic field. Traditional methods use volume integrals over the domains occupied by anomalous susceptibility and on the prismatic representation of the volumes with an anomalous susceptibility distribution. Such discretization is computationally expensive, particularly in 3-D cases. The technique of Cauchy-type integrals makes it possible to represent the magnetic field as surface integrals, which is particularly significant in solving problems of the modeling and inversion of magnetic data for the depth to the basement. In this letter, a novel method is proposed, which only requires discretizing the magnetic contrast surface for modeling and inversion. We demonstrate the method using several synthetic models. The results show that the new method is fast and capable of providing high-resolution depth estimation for the sediment–basement interface.

Index Terms—Basement depth, Cauchy-type integral, inversion, magnetic.

I. INTRODUCTION

MAGNETIC surveys serve as an important tool for the estimation of the depth to a crystalline basement [1]–[3]. The conventional magnetometers (e.g., fluxgate, induction coil, or optical pumping magnetometers [4]) can be used to conduct these surveys. The observed magnetic data contain the response from geological structures in multiple scales, and as such, the response from the magnetic basement can be masked in the observed data. However, sediments are usually formed by nonmagnetic rocks, whereas the rock formations of the basement have high magnetization, which makes it feasible to treat the observed data as a response from the crystalline basement only. In a general case, the localized shallow anomaly and a regional field caused by the effect of the basement

Manuscript received June 2, 2014; revised July 12, 2014; accepted August 7, 2014. This work was supported in part by the University of Utah’s Consortium for Electromagnetic Modeling and Inversion, by TechnoImaging, and by the Moscow Institute of Physics and Technology.

H. Cai is with the Consortium for Electromagnetic Modeling and Inversion, University of Utah, Salt Lake City, UT 84112 USA (e-mail: caihongzhu@hotmail.com).

M. S. Zhdanov is with the Consortium for Electromagnetic Modeling and Inversion, University of Utah, Salt Lake City, UT 84112 USA; with TechnoImaging, Salt Lake City, UT 84107 USA; and also with the Moscow Institute of Physics and Technology, Moscow 141700, Russia (e-mail: michael.s.zhdanov@gmail.com).

Color versions of one or more of the figures in this paper are available online at <http://ieeexplore.ieee.org>.

Digital Object Identifier 10.1109/LGRS.2014.2347275

can be separated using different separation methods or digital filters [5].

A conventional approach to solving the depth-to-basement magnetic inverse problem is based on the prism inversion of the subsurface [6] or on the Euler deconvolution method [7] to estimate the source properties. In the prism-based inversion, the subsurface is discretized into a grid of columns with known horizontal dimensions and known magnetic susceptibility. In the case where the average magnetic susceptibility profile with depth is well known, the magnetic data are a function of the depth to the basement, and the inversion can be applied for the thicknesses of the columns [8]. However, this method is computationally expensive for a large-scale problem.

Zhdanov and Cai [9] introduced a new method for the depth-to-basement modeling of a gravity field based on 3-D analogs of Cauchy-type integrals [10]–[13]. In this letter, we have extended this approach to magnetic field problems. We have developed an algorithm of the forward modeling of the magnetic field for a sediment–basement interface using the Cauchy-type integral approach. We have also developed an inversion scheme to estimate the depth to a magnetic basement using the new forward modeling method, which is based on the surface integration. The inversion algorithm is illustrated on a number of synthetic models of a crystalline basement.

II. PRINCIPLES OF MODELING AND INVERSION OF MAGNETIC FIELD USING CAUCHY-TYPE INTEGRALS

It was shown by Zhdanov [12] that the magnetic field, i.e., $\mathbf{H}(\mathbf{r}')$, due to a magnetized 3-D body with the intensity of magnetization $\mathbf{I}(\mathbf{r})$ can be represented by a 3-D analog of the Cauchy-type integral as follows:

$$\mathbf{H}(\mathbf{r}') = \mathbf{C}^S(\mathbf{r}', \mathbf{h}(\mathbf{r}) - \mathbf{h}(\mathbf{r}') - 4\pi\mathbf{I}_n(\mathbf{r})) \quad (1)$$

where the 3-D body is bounded by a closed surface S , $\mathbf{I}_n(\mathbf{r})$ is the projection of magnetization intensity $\mathbf{I}(\mathbf{r})$ on the normal direction, i.e., \mathbf{n} , to surface S , and $\mathbf{h}(\mathbf{r})$ is an arbitrary solution inside a 3-D domain of the following:

$$\nabla \cdot \mathbf{h} = 4\pi \nabla \cdot \mathbf{I} \quad \nabla \times \mathbf{h} = \mathbf{0}. \quad (2)$$

The intensity of magnetization is defined as the inducing geomagnetic field \mathbf{H}_l multiplied by magnetic susceptibility χ , which is the intrinsic property of rocks, i.e., $\mathbf{I}(\mathbf{r}) = \chi\mathbf{H}_l$.

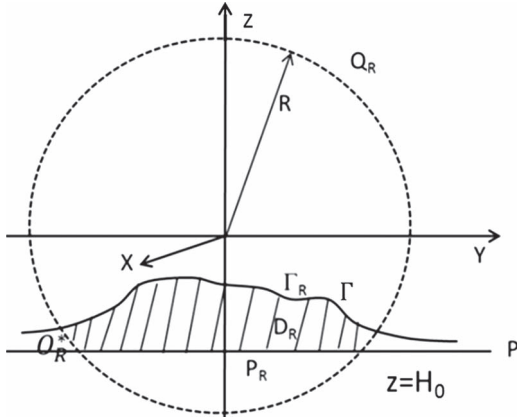


Fig. 1. Illustration of the sediment–basement interface model. The reference sediment–basement interface is a horizontal plane P , whereas the actual sediment–basement interface is surface Γ_R with $R \rightarrow \infty$.

In (1), term C^S represents a 3-D analog of the Cauchy-type integral defined as follows [12]:

$$C^S(\mathbf{r}', \varphi) = -\frac{1}{4\pi} \int \int_S \left[(\mathbf{n} \cdot \varphi) \nabla \frac{1}{|\mathbf{r} - \mathbf{r}'|} + (\mathbf{n} \times \varphi) \nabla \frac{1}{|\mathbf{r} - \mathbf{r}'|} \right] ds. \quad (3)$$

In scalar notations, a 3-D Cauchy-type integral is defined as

$$C_\alpha^S(\mathbf{r}', \varphi) = \frac{1}{-4\pi} \int \int_S \Delta_{\alpha\beta\gamma\eta} \varphi_\beta \frac{r'_\eta - r_\eta}{|\mathbf{r} - \mathbf{r}'|^3} n_\gamma ds \quad (4)$$

where each symbol $\alpha, \beta, \gamma, \eta$ can be equal to x, y, z , i.e., $\alpha, \beta, \gamma, \eta = x, y, z$, and the four-index Δ symbol is represented in terms of the Kronecker delta symbol, i.e., $\delta_{\alpha\eta}$, as follows:

$$\Delta_{\alpha\beta\gamma\eta} = \delta_{\alpha\eta} \delta_{\beta\gamma} + \delta_{\alpha\beta} \delta_{\gamma\eta} - \delta_{\alpha\gamma} \delta_{\beta\eta}. \quad (5)$$

Note that, in (4), we use an agreement on the summation that the twice-repeated index indicates the summation over this index.

If we consider a Laplacian distribution of the magnetization vector inside the 3-D domain, the magnetic field can be expressed using a Cauchy-type integral as follows:

$$\mathbf{H}(\mathbf{r}') = -4\pi C^S(\mathbf{r}', \mathbf{I}_n(\mathbf{r})). \quad (6)$$

For a more special case, where the magnetization vector is a constant inside domain D , we have

$$\mathbf{I}(\mathbf{r}) = \mathbf{I}^0. \quad (7)$$

In such a case, (6) can be written as follows:

$$\mathbf{H}(\mathbf{r}') = -4\pi C^S(\mathbf{r}', \mathbf{I}_n^0(\mathbf{r})). \quad (8)$$

Now, we consider a typical model of a sediment–basement interface. Surface Γ in Fig. 1 represents an actual sediment–basement interface, whereas a reference plane P characterizes the asymptotic behavior of Γ at infinity. Domain D is bounded by surface Γ and plane P . We will calculate the magnetic effect of domain D filled with magnetized material with magnetization vector \mathbf{I}^0 . To this end, we cut

from domain D a domain D_R bounded by a spherical surface Q_R with a radius R and the parts Γ_R and P_R of surfaces Γ and P cut therefrom by sphere Q_R (see Fig. 1). We assume that surface Γ_R tends to plane P at infinity. We consider a nonmagnetized sediment, which is typically the case, and a uniformly magnetized basement with magnetization vector \mathbf{I}^0 . In this case, the magnetic anomaly due to the basement can be calculated as the effect of the bounded domain D_R with $R \rightarrow \infty$.

According to (1), the magnetic field caused by the bounded domain D_R can be represented as follows:

$$\mathbf{H}(\mathbf{r}') = -4\pi \{ C^{\Gamma_R}(\mathbf{r}', \mathbf{I}_n^0(\mathbf{r})) + C^{Q_R^* \cup P_R}(\mathbf{r}', \mathbf{I}_n^0(\mathbf{r})) \} \quad (9)$$

where Q_R^* is a lateral surface of sphere Q_R enclosed between Γ and P . Since we assume that surface Γ tends to horizontal plane P , the integral over Q_R^* tends to zero when $R \rightarrow \infty$. Therefore, (9) can be reduced to the following form:

$$\mathbf{H}(\mathbf{r}') = -4\pi \{ C^{\Gamma_R}(\mathbf{r}', \mathbf{I}_n^0(\mathbf{r})) + C^{P_R}(\mathbf{r}', \mathbf{I}_n^0(\mathbf{r})) \} \quad (10)$$

with $R \rightarrow \infty$. The total magnetization vector \mathbf{I}^0 can be also decomposed into the vertical and horizontal components as follows:

$$\mathbf{I}^0 = \mathbf{I}_v^0 + \mathbf{I}_h^0. \quad (11)$$

It is easy to see that both the vertical and horizontal components are constant within domain D , and the vertical component of the magnetization vector is the same as the normal component of the magnetization vector on plane P_R .

Taking into account that \mathbf{I}_v^0 is the Laplacian vector inside of domain D and that point \mathbf{r}' is outside of D , we have

$$C^{\Gamma_R \cup P_R}(\mathbf{r}', \mathbf{I}_v^0) = 0 \quad (12)$$

which leads to the following result:

$$C^{P_R}(\mathbf{r}', \mathbf{I}_v^0) = -C^{\Gamma_R}(\mathbf{r}', \mathbf{I}_v^0). \quad (13)$$

By substituting (13) into (10) and taking into account that $R \rightarrow \infty$, we finally find that

$$\mathbf{H}(\mathbf{r}') = -4\pi C^\Gamma(\mathbf{r}', \mathbf{I}_n^0(\mathbf{r}) - \mathbf{I}_v^0). \quad (14)$$

In a geophysical exploration, one measures the total magnetic intensity (TMI) field, i.e., H_T , which is defined as follows:

$$H_T = \mathbf{l} \cdot \mathbf{H} = l_x H_x + l_y H_y + l_z H_z \quad (15)$$

where \mathbf{l} is a unit vector, which denotes the direction of the inducing geomagnetic field as follows:

$$\mathbf{l} = (l_x, l_y, l_z). \quad (16)$$

By substituting formula (4) into (14), we can find the expressions of the scalar components of the magnetic field caused by the sediment–basement interface as follows:

$$H_\alpha(\mathbf{r}') = \int \int_\Gamma \Delta_{\alpha\beta\gamma\eta} (\mathbf{I}_n^0(\mathbf{r}) - \mathbf{I}_v^0)_\beta \frac{r'_\eta - r_\eta}{|\mathbf{r} - \mathbf{r}'|^3} n_\gamma ds. \quad (17)$$

We define the distance between the actual sediment–basement interface and reference plane $P(z = H_0)$ as follows:

$$h = z - H_0. \quad (18)$$

Using the property of the four-index Δ symbol in (5), after some algebra, we find that the scalar components of the magnetic field (taking H_z for example) can be represented by the following surface integrals:

$$H_z(\mathbf{r}') = \iint_{\Gamma} \frac{1}{|\mathbf{r} - \mathbf{r}'|^3} \left\{ (z' - z) [\mathbf{I}_n^0(\mathbf{r})_x b_x + \mathbf{I}_n^0(\mathbf{r})_y b_y + \mathbf{I}_n^0(\mathbf{r})_z] - I_v^0 [(x' - x)b_x + (y' - y)b_y + (z' - z)] \right\} dx dy \quad (19)$$

where

$$b_x = -\frac{\partial h}{\partial x} \quad b_y = -\frac{\partial h}{\partial y} \quad b_z = 1. \quad (20)$$

The TMI can be computed using expression (15) and the formula for the scalar components of the magnetic field.

We discretize the surface integrals for computing the magnetic field by dividing horizontal plane XY into a grid of N_m cells with constant discretization sizes of Δx and Δy in the x - and y -directions, respectively, and by representing the contrast surface using elevations $h^{(k)} = h(x_k, y_k)$ above reference plane P . As a result, within each cell $P_k (k = 1, 2, \dots, N_m)$, the corresponding magnetization contrast surface can be represented by a flat plane described by the following linear equation:

$$z = h^{(k)} - b_x^{(k)}(x - x_k) - b_y^{(k)}(y - y_k) + H_0 \quad (21)$$

where (x_k, y_k) denotes the center of the cell.

In a discretized form, the TMI caused by the sediment–basement interface can be written as follows:

$$H_T(\mathbf{r}'_n) = \sum_{k=1}^{N_m} f_T^{nk} \quad (22)$$

where the kernel is defined as follows:

$$\begin{aligned} f_T^{nk} &= \frac{\Delta x \Delta y}{|\mathbf{r}_k - \mathbf{r}'_n|^3} [\mathbf{I}_{nx}^0(\mathbf{r}_k) b_x^k + \mathbf{I}_{ny}^0(\mathbf{r}_k) b_y^k + \mathbf{I}_{nz}^0(\mathbf{r}_k)] \\ &\times [l_x (x'_n - x_k) + l_y (y'_n - y_k) + l_z (z'_n - z_k)] + I_v^0(\mathbf{r}_k) \\ &\times [(z'_n - z_k) (l_x b_x^k + l_y b_y^k - l_z) - (x'_n - x_k) \\ &\times (l_x + l_z b_x^k) - (y'_n - y_k) (l_y + l_z b_y^k)]. \quad (23) \end{aligned}$$

In the inversion, we consider the elevations of the contrast surface as unknown model parameters. This inverse problem is an ill-posed and nonlinear problem, whereas the traditional magnetic inversion to recover the susceptibility distribution is a

linear problem. We apply the Tikhonov regularization method for solving the inverse problem [14]. This method is based on the minimization of the Tikhonov parametric functional consisting of the misfit and stabilizing functionals, which is defined in a matrix notation as follows [15]:

$$P(\mathbf{m}) = (W_d A(\mathbf{m}) - W_d \mathbf{d})^T (W_d A(\mathbf{m}) - W_d \mathbf{d}) + (W_m \mathbf{m} - W_m \mathbf{m}_{\text{apr}})^T (W_m \mathbf{m} - W_m \mathbf{m}_{\text{apr}}) \quad (24)$$

where W_d is the data weighting matrix, A is the forward modeling operator, \mathbf{m} is the model vector, \mathbf{d} is the data vector, W_m is the model weighting matrix based on the integrated sensitivity [15], and \mathbf{m}_{apr} is the *a priori* model. The *a priori* model is used to incorporate information about the model that might be available from other geophysical surveys and/or geological data [16], [17]. The selection of a suitable initial model can speed up the inversion and help recovering the most reasonable inverse model. In our model study, however, we assume that no *a priori* model is available, and we use horizontal reference plane H_0 as the initial model of the top of the basement. We have also found by numerical experiments that the inversion method is robust with respect to the selection of the initial model.

The minimization of the corresponding Tikhonov parametric functional is based on the reweighted regularized conjugate gradient method [15]. Although this inversion problem is a nonlinear problem, the Fréchet derivative operator can be analytically evaluated by taking the derivatives of the forward modeling operator represented by Cauchy-type integrals with respect to the model parameter.

For example, in order to compute the Fréchet derivative of the TMI operator, we take the derivative of expression (22) with respect to model parameter h_l . For simplicity, we approximate the magnetization contrast surface with a series of piecewise horizontal surfaces with $b_x = b_y = 0$. After some algebra, we can find the Fréchet derivative for the TMI operator in the discretized form as (25), shown at the bottom of the page.

The developed theory and method have been implemented in a computer code, which was tested on several synthetic models, as discussed in the following.

III. MODEL STUDIES

In this section, we present a model study of the modeling of the TMI data caused by the sediment–basement interface. We assume that horizontal reference plane P is located at a depth of 1000 m under the Earth's surface. The sediment–basement interface, with the minimum elevation of -1300 m, is below horizontal plane P . The forward modeling results based on the Cauchy-type integral approach are compared with the results obtained using the traditional prismatic discretization.

Fig. 2 shows the synthetic model with the actual sediment–basement interface placed below reference plane $P (= -1000$ m). The observation stations are located at the Earth's surface at $z = 0$. We consider the vertical magnetization of

$$F_{nl} = \frac{(\mathbf{I}_n^0(\mathbf{r})_z - \mathbf{I}_v^0) \Delta x \Delta y}{|\mathbf{r}_l - \mathbf{r}'_n|^3} \left\{ \frac{3(h_l + H_0 - z'_n) [l_z (h_l + H_0 - z'_n) - l_x (x'_n - x_l) - l_y (y'_n - y_l)]}{|\mathbf{r}_l - \mathbf{r}'_n|^2} - l_z \right\} \quad (25)$$

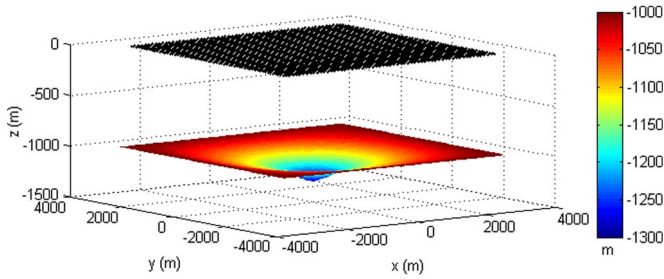


Fig. 2. Realistic model of the sediment–basement interface with the negative anomaly. The lower surface is the actual boundary between the sediments and the basement. The black dots are the observation stations for recording the magnetic response.

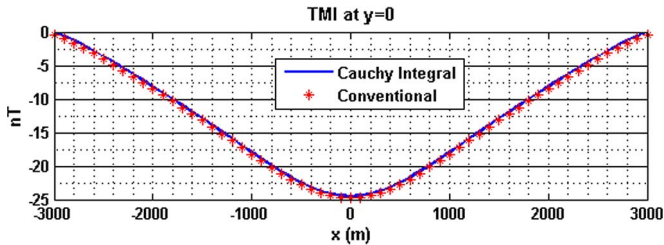


Fig. 3. Comparison of the TMI data computed using the Cauchy-type integral approach and the conventional method for the synthetic model.

the inducing field with a magnitude of 60 000 nT. We assume that the sediment is nonmagnetized, whereas the basement is uniformly magnetized with a magnetic susceptibility of 0.01 in SI units. Fig. 3 presents a comparison of the TMI data computed using the Cauchy-type integral and the conventional method at $y = 0$. One can see in this figure that the fields computed using these two methods practically coincide. We should note that the new method is very fast. In our numerical study, the computation of the TMI field using the Cauchy-type integral method was almost 60 times faster than by the traditional volume integral method.

IV. INVERSION OF ENSENADA BAY MAGNETIC DATA

We present the results of the inversion of the magnetic data for the Ensenada Bay sediment–basement interface model. Ensenada Bay is located off a peninsula of Baja California. The area is characterized by a relatively shallow basement. Structurally, the basin is controlled by the active South and North Agua Blanca faults [8].

Several gravity and magnetic surveys were conducted in this area for regional geological studies. Gallardo *et al.* [8] performed a joint inversion of gravity and magnetic data for the depth-to-basement surface. Since we do not have access to the data in this area, we just reconstructed a 3-D model of the sediment–basement interface using a 2-D geological section from the work in [8] (see Fig. 4). Fig. 5 shows the reconstructed 3-D model. The left portion of the sediment–basement interface is above reference plane P , whereas the right portion is below plane P . For this model, we assume a vertical magnetization of the basement. According to [8], the magnetic susceptibility of the sediment is 0, and the magnetic susceptibility of the basement is 0.01 in SI units.

We simulated the TMI data using a computer with 5% random noise added. The simulated data were used as synthetic observed data for inversion.

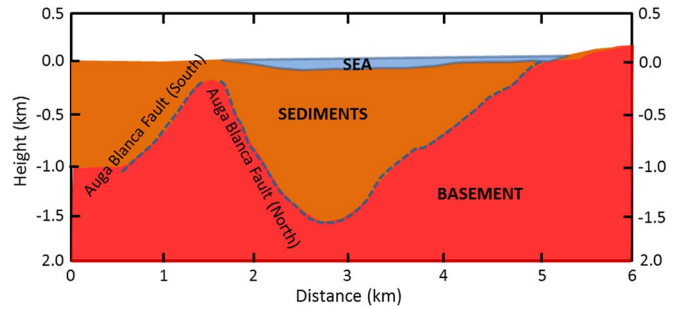


Fig. 4. Two-dimensional cross section showing the basement, the sedimentary basin, the bathymetry, and the topography of Ensenada Bay (modified after [8]).

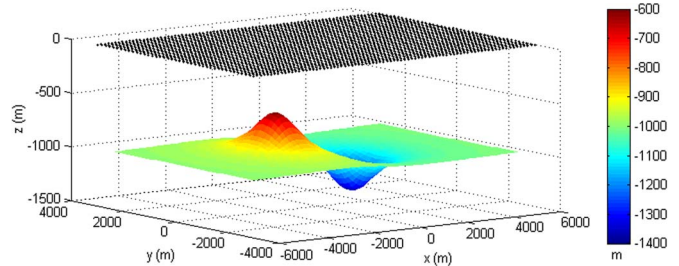


Fig. 5. Reconstructed 3-D model of the Ensenada Bay basement. The reference plane for this model is a horizontal plane located at -1000 m. The black dots are the observation stations for recording the magnetic response.

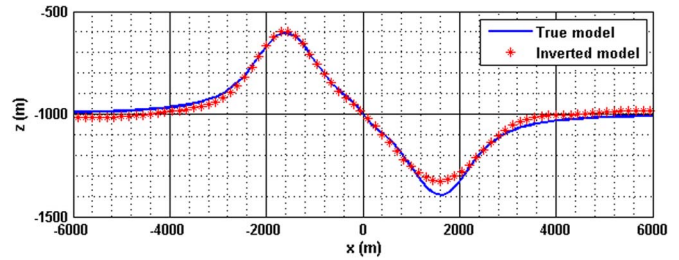


Fig. 6. Comparison between the true sediment basement interface and the interface recovered from the inversion for the Ensenada Bay model at $y = 0$.

Our inversion converged to a tolerance of 5%, which is the noise level of the data after just a few iterations. Fig. 6 presents a comparison of the true model and the inversion result at $y = 0$. We can see that the depth to the basement is recovered well, particularly in the left part where the actual sediment–basement interface is shallower than reference plane P . In the right part, the recovered depth to the basement is slightly underestimated. This can be explained by the decrease in the sensitivity of the data to the basement as the depth increases. This problem can be overcome by adding additional *a priori* information about the depth to the basement from drilling or from other geophysical data, e.g., from gravity, electromagnetic, and seismic surveys, if they are available [18], [19].

V. INVERSION OF MAGNETIC DATA FOR BIG BEAR LAKE BASIN MODEL

We will consider the inversion of the magnetic data for the Big Bear Lake Basin model. The area is located at the south part of California, and it is characterized by a deep sediment basin with the depth up to several kilometers and with several fault structures. The geological structure and basin geometry of

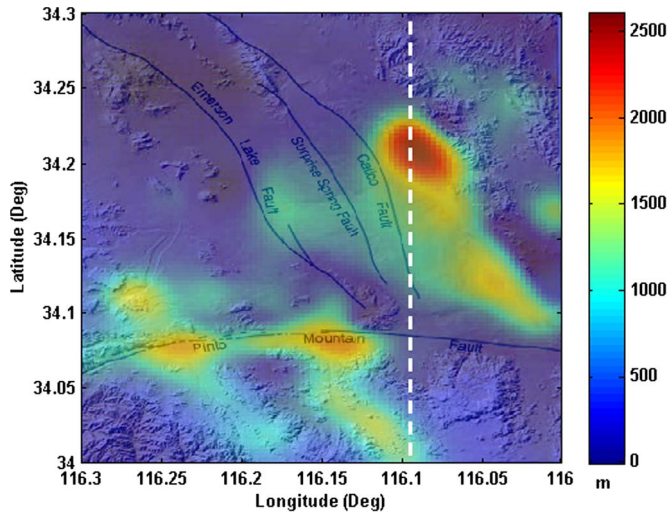


Fig. 7. USGS Big Bear Lake Basin model. The color map shows the depth to the basement. The white line is the profile at which our inversion result is compared with the true model.

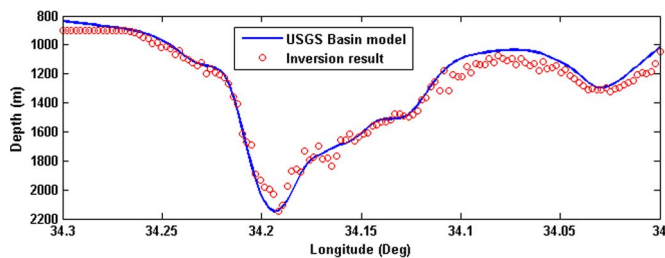


Fig. 8. Comparison of the inversion result with the USGS Big Bear Lake Basin model along the latitude of 116.09° .

this area is well known based on integrated geophysical data interpretation [18].

We simulated the synthetic magnetic data based on the basin model recovered from the USGS gravity data inversion [18]. Fig. 7 shows the USGS Big Bear Lake Basin model overlapped with surface geology. We can clearly see the shape of the basin and four major fault structures in this figure.

We consider a nonmagnetized sediment and a uniform magnetized basement with a magnetic susceptibility of 0.01 in SI units, which is similar to the Ensenada Bay model. We have applied our inversion algorithm to the synthetic magnetic data in order to estimate the depth to the basement. Fig. 8 shows a comparison of the recovered depth to the basin and the true depth along the white line shown in Fig. 7. In this figure, we can see that the recovered depth to the basin has good agreement with the true basin model.

VI. CONCLUSION

We have developed novel methods of the forward modeling and inversion of magnetic data based on 3-D analogs of Cauchy-type integrals. We have illustrated these methods by modeling the magnetic anomaly effect due to the sediment-basement interface with contrast magnetization. In our modeling process, we only discretized the magnetization contrast surface, which resulted in the significant reduction of the

amount of computations compared with traditional methods based on volume discretization. We have also applied the developed method to solve the inverse problem of recovering the location of the magnetic contrast surface. This inverse problem is nonlinear and is ill-posed. We consider a minimization of the Tikhonov parametric functional in order to solve this ill-posed inverse problem. The Fréchet derivative matrix is analytically computed by the differentiation of the forward modeling operator represented by the Cauchy-type integrals. Our model study demonstrates that the depth to the magnetic basement can be recovered well by our methods.

ACKNOWLEDGMENT

The authors would like to thank Dr. Gallardo for providing the Ensenada Bay basin information and the USGS for the release of the Big Bear Lake Basin model.

REFERENCES

- [1] M. V. Rybakov and A. Segev, "Top of the crystalline basement in the Levant," *Geochem., Geophys., Geosyst.*, vol. 5, no. 9, pp. 1–8, Sep. 2004.
- [2] V. Tschirchart *et al.*, "3-D geophysical inversion of the north-east Amer Belt and their relationship to the geologic structure," *Geophys. Prospecting*, vol. 61, no. S1, pp. 547–560, Jun. 2013.
- [3] A. Salem *et al.*, "Sedimentary basins reconnaissance using the magnetic tilt-depth method," *Exploration Geophys.*, vol. 41, no. 3, pp. 198–209, Sep. 2010.
- [4] M. S. Zhdanov, *Geophysical Electromagnetic Theory and Methods*. Amsterdam, The Netherlands: Elsevier, 2009.
- [5] Y. Li and D. Oldenburg, "Separation of regional and residual magnetic field data," *Geophysics*, vol. 63, no. 2, pp. 431–439, Mar./Apr. 1998.
- [6] J. D. Phillips, "Potential-Field Geophysical Software for the PC version 2.2," U.S. Dept. Interior, U.S. Geol. Survey, Denver, CO, USA, 1997.
- [7] G. Martelet, J. Perrin, C. Truffert, and J. Deparis, "Fast mapping of magnetic basement depth, structure and nature using aeromagnetic and gravity data: Combined methods and their application in the Paris basin," *Geophys. Prospecting*, vol. 61, no. 4, pp. 857–873, Jul. 2013.
- [8] L. A. Gallardo, M. A. Perez, and E. G. Treviño, "A versatile algorithm for joint 3D inversion of gravity and magnetic data," *Geophysics*, vol. 68, no. 3, pp. 949–959, May 2003.
- [9] M. S. Zhdanov and H. Cai, "Inversion of gravity and gravity gradiometry data for density contrast surfaces using Cauchy-type integral," in *Proc. SEG Annu. Meet.*, 2013, pp. 1161–1165.
- [10] M. S. Zhdanov, "Use of Cauchy integral analogs in the geopotential field theory," *Ann. Geophys.*, vol. 36, no. 4, pp. 447–458, 1980.
- [11] M. S. Zhdanov, *Cauchy Integral Analogs in Geophysical Field Theory*. Moscow, Russia: Nauka, 1984, (in Russian).
- [12] M. S. Zhdanov, *Integral Transforms in Geophysics*. Berlin, Germany: Springer-Verlag, 1988.
- [13] M. S. Zhdanov and X. Liu, "3-D Cauchy-type integrals for terrain correction of gravity and gravity gradiometry data," *Geophys. J. Int.*, vol. 194, no. 1, pp. 249–268, Jul. 2013.
- [14] A. N. Tikhonov and V. Y. Arsenin, *Solutions of Ill-posed Problems*. Washington DC, DC, USA: V. H. Winston and Sons, 1977.
- [15] M. S. Zhdanov, *Geophysical Inverse Theory and Regularization Problems*. Amsterdam, Netherlands: Elsevier, 2002.
- [16] Y. Li and D. Oldenburg, "3-D inversion of magnetic data," *Geophysics*, vol. 61, no. 2, pp. 394–408, Mar./Apr. 1996.
- [17] H. Rim, Y. Park, M. Lim, S. Koo, and B. Kwon, "3-D gravity inversion with Euler deconvolution as *a priori* information," *Exploration. Geophys.*, vol. 38, no. 1, pp. 44–49, 2007.
- [18] C. Roberts, R. Jachens, A. Katzenstein, G. Smith, and R. Johnson, "Gravity map and Data of the Eastern Half of the Big Bear Lake, 100,000 Scale Quadrangle," U. S. Geol. Survey, Reston, VA, USA, Open-File Rep. 02–353, 2002.
- [19] P. Lelièvre, C. Farquharson, and C. Hurich, "Joint inversion of seismic travel times and gravity data on unstructured grids with application to mineral exploration," *Geophysics*, vol. 77, no. 1, pp. K1–K15, 2012.